Oxidation-Induced Ligand Swap: Oxygen Insertion into a Cobalt-Phosphine Complex

Sriram Katipamula, Thomas J. Emge, Kate M. Waldie*

Department of Chemistry and Chemical Biology, Rutgers, The State University of New Jersey, Piscataway, New Jersey 08854, United States

*kate.waldie@rutgers.edu

ABSTRACT

The synthesis and characterization of a half-sandwich cobalt(II) complex supported by the bidentate, pendent-amine phosphine ligand ($P^{Ph}_2N^{Bn}_2$ = 1,5-diaza-3,7-diphosphacyclooctane) are reported. Oxidation of a cobalt(I)-phosphine precursor with silver(I) salts yielded the paramagnetic complex $[CpCo(P^{Ph}_2N^{Bn}_2)]^+$. This species rapidly reacts with oxygen upon air exposure under ambient conditions, resulting in the insertion of oxygen into the cobalt-phosphine bonds. Two cobalt complexes were generated from this reaction: the cobaltocenium cation, bearing two Cp ligands (Cp = cyclopentadienyl); and a cobalt(II)-bis(phosphine oxide) dicationic complex in which two $O_2P_2N_2$ ligands coordinate in a *fac* fashion via two oxygen and one nitrogen centers to establish an overall octahedral geometry. Thus, the aerobic oxidation of the phosphine induces the exchange and rearrangement of the ligands at cobalt.

INTRODUCTION

Phosphine ligands are ubiquitous in organometallic complexes and feature prominently in coordination chemistry and catalysts.[1-4] Ligand scaffolds based on phosphine donors offer tunable steric and electronic properties through variations of the phosphine substituents, allowing for the optimization of the ancillary ligand properties and opening the door to the introduction of pendent functionalities that actively participate in substrate reactivity.[5-8] However, one challenge associated with phosphine ligands and their transition metal complexes is their potential oxygen sensitivity; exposure to air can lead to catalyst decomposition and the formation of intractable mixtures.[9-10] This issue is particularly detrimental for transition-metal catalyzed reactions that

utilize oxygen or air as the terminal oxidant. Given the advantages of using O_2 as a sustainable reagent in favor of more hazardous chemical oxidants[11-14] and significant role that oxygenation reactions play in chemical and biological processes,[15-18] understanding the reactivity of transition metal-phosphine complexes in the presence of oxygen has broad implications for homogeneous catalysis. Furthermore, oxygen tolerance is crucial for catalytic or electrocatalytic applications under practical conditions, and identifying aerobic degradation pathways can inform strategies to improve catalyst activity and lifetimes.[19-20]

Half-sandwich complexes based on cobalt(III) represent a well-studied class of complexes that have been explored for several decades.[21] Within this family, a variety of different monodentate and bidentate phosphine scaffolds have been employed as ancillary ligands.[22-29] In general, [$CpCo^{III}$] complexes exhibit a pseudo-octahedral geometry based on the *fac*-type Cp ring (Cp = cyclopentadienyl) in conjunction with three additional ligand coordination sites. These diamagnetic complexes are largely reported to be air-stable thanks to their robust coordination geometry, low-spin d^6 metal center, and mild redox potentials. Nonetheless, catalytic reactions are generally conducted under inert atmosphere due to the anticipated or known oxygen sensitivity of proposed reaction intermediates, particularly low-valent complexes; however, their reactivity with O_2 has not been described.

In the course our studies with CpCo-phosphine complexes,[28-29] we have reported several $[CpCo^{III}(P\text{-}P)(X)]^{n+}$ (X = MeCN, H^-) and $[CpCo^{I}(P\text{-}P)]$ complexes, which exhibit comparable structural and electrochemical properties to related systems reported by other groups.[22-27] The coordination geometry at cobalt differs depending on the metal oxidation state: unlike the Co^{III} complexes, the Co^{I} systems have a two-legged piano stool geometry (Figure 1a). There are few examples of $CpCo^{II}$ complexes in this family, and these structures also exhibit the two-legged piano stool geometry in the solid state,[28, 30-31] which may open the door to substrate coordination and reactivity at the coordinatively-unsaturated metal center. Herein, we report the synthesis and characterization of the [$CpCo^{II}$] complex **1** supported by a bidentate P_2N_2 ligand (P_2N_2 = 1,5-diaza-3,7-diphosphacyclooctane; Figure 1b). This complex undergoes rapid reaction with oxygen upon exposure to air to form the six-coordinate octahedral complex **2** in which the phosphine ligand has been oxidized to the phosphine oxide. The Cp ligand is lost from this structure and undergoes a ligand exchange process, leading to the formation of the cobaltocenium cation (Cp_2Co^+) as the co-product of this reaction.

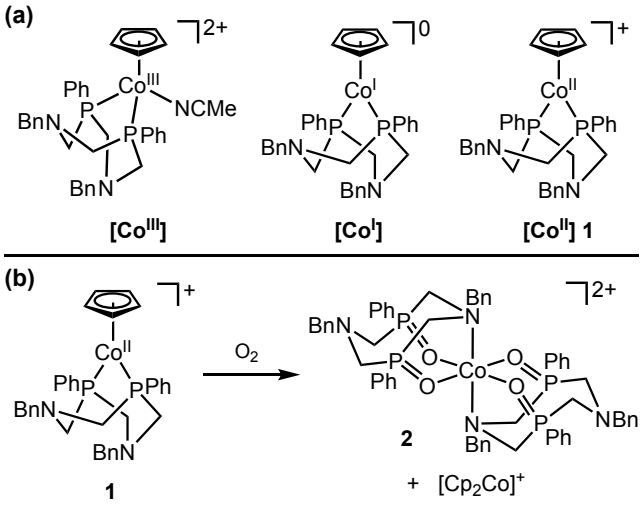

Figure 1. (a) Structures of CpCo-P_2N_2 complexes in the Co^{III}, Co^{I}, and Co^{II} states. (b) Aerobic oxidation of **1**.

RESULTS AND DISCUSSION

Synthesis and Characterization of [Co^{II}] 1

In principle, complex **1** can be accessed via three different synthetic routes: one-electron reduction of the [Co^{III}] complex, one-electron oxidation of the [Co^{I}] complex, or comproportionation of [Co^{III}] and [Co^{I}] (Scheme 1a). While **1** can indeed be prepared by each of these approaches, the second route through oxidation of [Co^{I}] gave the most reproducible results in our hands. Thus, to obtain complex **1**, we first synthesized [Co^{III}] and then [Co^{I}] following our previously established procedures.[29] Next, the [Co^{I}] complex was oxidized by treatment with 0.9 eq. silver hexafluorophosphate ($AgPF_6$) in acetonitrile. This reaction is fast, and **1** is obtained as a green solid within 5 min (Scheme 1b). Following recrystallization from a saturated acetonitrile/diethyl ether solution, **1** is isolated in moderate yield (42%). We note that the use of less than one equivalent of $AgPF_6$ is highly beneficial for purification of the final product, as this procedure ensures that the chemical oxidant is fully consumed in the reaction, and any unreacted [Co^{I}] is readily removed from **1** recrystallization due to its high solubility in nonpolar solvents. Complex **1** must be handled under an inert atmosphere (*vide infra*) but is otherwise reasonably stable in solution or the solid state.

Scheme 1. (a) Viable routes to prepare [Co^{II}] **1**. (b) Synthesis of [Co^{II}] **1**.

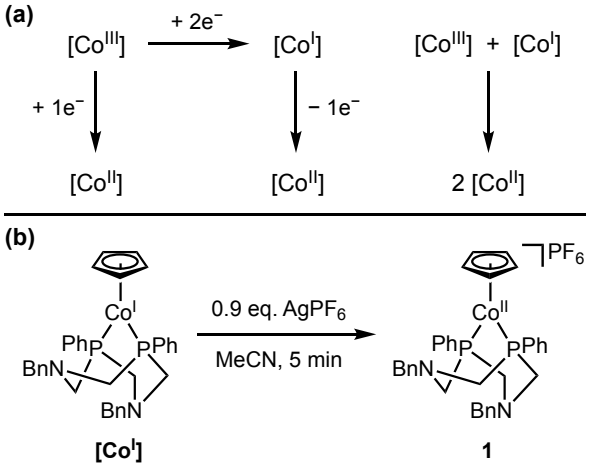

The starting [Co^{I}] complex is diamagnetic and shows clearly resolved ^{1}H and ^{31}P NMR signals.[29] As expected, one-electron oxidation of this complex to [Co^{II}] **1** results in a paramagnetic species. This is evident from the ^{1}H NMR analysis of **1** in CD_3CN, which shows multiple paramagnetically broadened resonances (Figure S3). It is difficult to confidently assign these broad signals to specific hydrogen atoms in the molecule, but we note that the approximate chemical shift range for **1** is comparable to other [$CpCo^{II}$] complexes featuring phosphine ligands.[24, 28] The ^{31}P NMR spectrum of **1** only shows the diagnostic septet signal for the hexafluorophosphate anion at δ_P –144.64 ppm. The absence of detectable ^{31}P signal for the P_2N_2 ligand is not surprising for a paramagnetic metal complex. The paramagnetism of **1** was further probed using Evans NMR method, from which the magnetic moment of **1** in solution was determined by to 1.84 μB at 25°C (Figure S4). This value is consistent with an S = ½ system and indicates that **1** is best formulated as a low-spin d^7 Co^{II} complex.

X-Ray quality crystals of **1** were grown by vapor diffusion of diethyl ether into a concentrated acetonitrile solution at −35°C. The structure of **1** is presented in Figure 2, and select structural metrics are provided in the Supporting Information. Complex **1** adopts a two-legged piano stool geometry with a planar η^5-Cp ligand and the bidentate phosphine ligand. The Co−P bond lengths are 2.157(2) and 2.155(2) Å, and the P−Co−P angle is 85.73(6)°. Broadly speaking, the structural metrics of **1** are similar to those of other reports of [$CpCo^{II}$] diphosphine complexes.[24, 30] Wiedner and co-workers reported a series of related [$^{R}CpCo^{II}(P^{tBu}{}_2N^{Ph}{}_2)$]$^{+}$ complexes where the Cp ligand contains R = H or electron-withdrawing substituents.[24] All

complexes, including **1**, have one P_2N_2 ring in the chair conformation and the other ring in the boat conformation in the solid-state structures, although the ligand conformation is fluxional in solution. The Co−P bond distances are slightly longer in Wiedner's complexes compared to **1** (by ca. 0.3-0.5 Å), which is likely due to the increased steric bulk of the t-butyl phosphine substituents in comparison to the phenyl substituents in **1**.

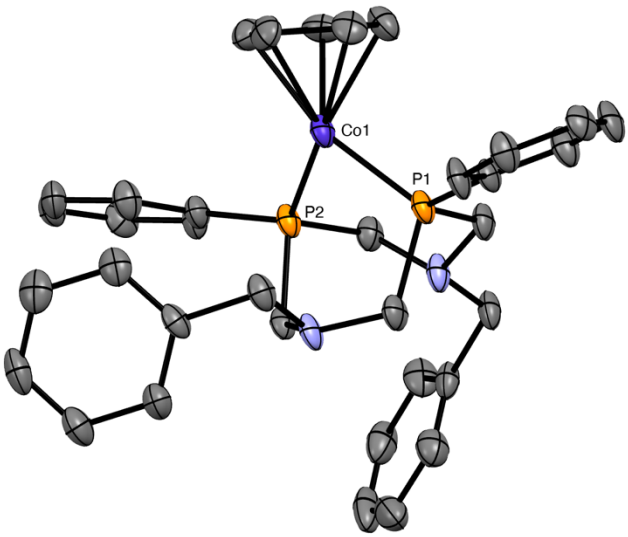

Figure 2. Structure of **1**. Hydrogen atoms and PF_6^- counterion are omitted for clarity. Ellipsoids shown at 50% probability.

The electrochemical properties of **1** were confirmed by cyclic voltammetry (CV) studies in acetonitrile using 0.1 M [^{n}NBu$_4$][PF_6] as the supporting electrolyte. All redox potentials are reported relative to the ferrocene/ferrocenium ($Fc^{+/0}$) redox couple as an internal standard. Complex **1** exhibits two reversible redox couples at −0.63 and −1.21 V vs $Fc^{+/0}$ (Figures 3 and S26). These features are assigned as the Co^{III}/Co^{II} couple for one-electron oxidation of **1** to [Co^{III}], and the Co^{II}/Co^{I} couple for one-electron reduction of **1** to [Co^{I}]. These assignments align with the well-established electrochemical behavior of related [CpCo] complexes in acetonitrile.[24, 26-28, 31] Furthermore, the potentials for both redox couples of **1** show excellent agreement comparing to the reported electrochemical properties of [Co^{III}].[25, 29] In addition, the open-circuit potential (OCP) for the electrochemical solution of **1** is approximately −0.90 V vs $Fc^{+/0}$, which lies between the Co^{III}/Co^{II} and Co^{II}/Co^{I} redox potentials. Thus, this value further corroborates that the bulk solution exists in the Co^{II} oxidation state.

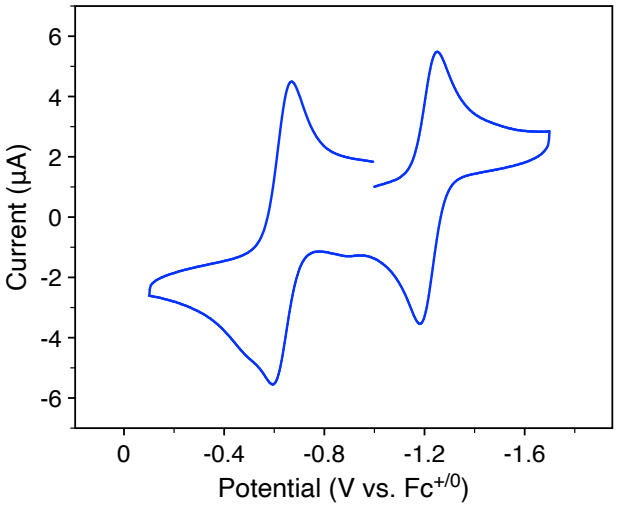

Figure 3. CV of **1** in MeCN (0.5 mM [**1**] and 0.1 M [^{n}Bu$_4$N][PF$_6$]; scan rate 100 mV/s).

Aerobic Oxidation of [Co^{II}] 1 to Prepare Complex 2

Treatment of the [Co^{II}] complex **1** with traditional chemical oxidants or an electrochemical potential in acetonitrile results in a metal-centered, one-electron oxidation and acetonitrile coordination to yield [Co^{III}].[26-27, 29] In contrast, we find significantly different reactivity when complex **1** is exposed to oxygen. In an initial experiment, an NMR solution of **1** in CD_3CN was opened to air, resulting in an immediate color change from green to dark orange. The ^{1}H NMR spectrum of the resulting solution reveals the complete loss of resonances associated with **1** and the emergence of new paramagnetically broad resonances spanning a large chemical shift range from –80 to +65 ppm (Figures S5 and S6). New diamagnetic signals are also observed. The sharp singlet at δ_H 5.67 ppm is consistent with the cobaltocenium cation (Cp_2Co^+), while other diamagnetic resonances around δ_H 3.5 and 7.0-7.7 ppm, which become more significant over time (Figure S8), are assigned as an uncoordinated phosphine oxide ligand (*vide infra*). The ^{31}P NMR displays two signals at δ_P 33.90 (s) and–144.62 (sept) ppm, attributed to the free phosphine oxide ligand and the hexafluorophosphate anion, respectively (Figure S7). Overall, these results suggest that **1** undergoes a rapid aerobic transformation into a new paramagnetic species and the cobaltocenium cation, with some degree of ligand dissociation. Repeating this experiment in the presence of an internal standard, the ^{1}H NMR yield of Cp_2Co^+ is ca. 30% relative to **1**, and ca. 30% of the ligand exists as the free oxide. There is no evidence of the free phosphine P_2N_2 ligand in the NMR spectra.

The presence of the cobaltocenium cation is evident in the ^{1}H NMR spectrum of this product. Nonetheless, single crystals of [Co^{II}-PO] **2** suitable for X-Ray crystallography were obtained by layering diethyl ether upon this CD_3CN NMR solution at –22°C. As seen in Figure 4, the structure of **2**, formulated as $[Co(O_2P^{Ph}{}_2N^{Bn}{}_2)_2][PF_6]_2$, bears little resemblance to the starting [CpCo] complex **1**. Complex **2** exhibits an octahedral geometry with two tridentate, *fac*-type ligands, and the Cp ligand has been entirely lost from the coordination sphere. The tridentate ligands are derived from aerobic oxidation of the P_2N_2 phosphines to the corresponding phosphine oxide. Each ligand coordinates to the cobalt center via the two oxygen atoms, while the pendent amine arms are oriented such that one amine group from each ligand interacts with the metal to establish the octahedral coordination environment. The insertion of oxygen into the Co-phosphorus bonds extends the length of the chelate backbone to form eight-membered metallocycle rings, which provides sufficient structural flexibility for the ligand to adopt a *fac* arrangement. The presence of two PF_6^- anions per cobalt in the crystal lattice confirms a Co^{II} oxidation state. The absence of the Cp ligand in **2** and the co-generation of Cp_2Co^+ from the oxidation of **1** suggests that this reaction involves a ligand exchange process, whereby two equivalents of **1** are converted into one equivalent each of the phosphine oxide-only and Cp-only products, **2** and Cp2Co$^+$, respectively.

The cobalt lies on an inversion center in the crystal structure. The Co−O bond lengths are 2.0359(9) and 2.0590(10) Å, and the O1−Co−O2 angle is 87.74(4)°. The *trans* angles for O1−Co−O1` and O2−Co−O2` are both 180°, indicating the ideal planarity of the equatorial coordination sites with the phosphine oxide ligands. The P−O bond lengths are 1.5062(9) and 1.5090(9). Broadly speaking, these distances are typical of Co^{II}−O=P bond lengths in the CCDC database, including for octahedral geometries.[32-41] Both Co−N bond lengths are 2.2722(11) Å, which are ca. 0.21-0.23 Å longer in comparison to the Co−O bonds. A wide range of Co^{II}-tertiary amine bond distances have been reported in the literature, generally varying from 2.0-2.3 Å for six-coordinate complexes; thus, the elongation in **2** is not considered substantial. DuBois and co-workers previously reported an isostructural nickel system $[Ni(O_2P^{Ph}{}_2N^{Bn}{}_2)_2][BF_4]_2$, denoted here as [$Ni^{II}$-PO], which was also characterized by X-ray crystallography.[42] This species was obtained by exposing the corresponding $[Ni(P^{Ph}{}_2N^{Bn}{}_2)_2]^{2+}$ complex to H_2 gas, followed by air. In [Ni^{II}-PO], the phosphine oxides occupy the equatorial plane, with Ni−O bond lengths within 0.015 Å of those for **2**. Two of the pendent amine groups are similarly coordinated to the metal center in [Ni^{II}-PO];

however, there is a noticeable difference in the M−N bond lengths, where the Ni−N bond lengths are appreciably shorter (2.172(2) and 2.180(2) Å).

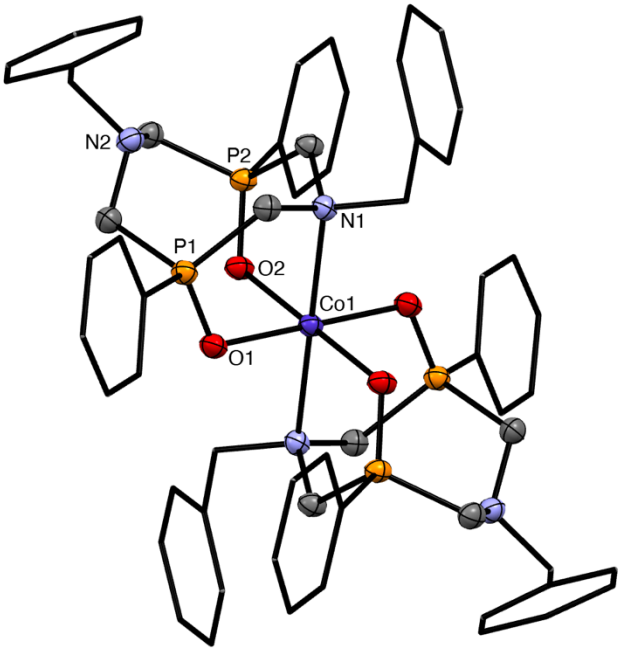

Figure 4. Structure of **2**. Hydrogen atoms, co-crystallized acetonitrile, and PF_6^- counterions are omitted for clarity. The phosphine and amine substituents are shown as capped sticks for clarity. Ellipsoids shown at 50% probability.

Complex **2** can also be reproducibly prepared on a larger scale following a similar procedure as described above: an acetonitrile solution of **1** was exposed to air and stirred for 5 min at 25°C. A rapid color change from green to orange was again observed. The crude product was recrystallized from a saturated acetonitrile/diethyl ether solution, yielding the mixture of **2** and Cp_2Co^+ as a yellow powder. NMR characterization of this isolated product matches the paramagnetic features obtained by *in-situ* oxidation (Figures S9 and S10). Recrystallization is effective for removing most of the diamagnetic impurities, but we are unable to separate the cobaltocenium cation from **2** due to the very similar solubilities of these species and the limited stability of **2** in solution. As mentioned briefly above, the diamagnetic species (not including Cp_2Co^+) become more significant over several hours when **2** is left in solution. This species is assigned as the free phosphine oxide ligand, which can be independently obtained by reduction of **2** with excess KC_8 (Figures S13 and S14). Thus, the phosphine oxide appears to be a weakly

coordinating ligand for the Co^{II} center and rather quickly dissociates from the metal in solution. The instability of **2** likely stems from the increased flexibility of the oxidized ligand resulting in a weaker chelate effect, as well as from the weaker donating abilities of the neutral oxygen and tertiary amine sites. Overall, these factors likely contribute to the lability of the coordination bonds, especially in the presence of coordinating solvents.

We note that the phosphine oxide ligand is not cleanly obtained by the direct oxidation of the P_2N_2 ligand by air. Instead, a mixture of unidentified products is observed by ^{31}P NMR (Figure S15). Alkyl phosphines typically yield multiple products upon reaction with oxygen due to uncontrolled radical pathways and oxygen insertion into several phosphorus-carbon bonds.[10, 43] Clearly, the coordination of the P_2N_2 ligand to the cobalt center in **1** enables its selective aerobic oxidation to the phosphine oxide.

In addition to simple recrystallization, we made several attempts to remove the Cp_2Co^+ co-product from **2** using chemical methods. We postulated that *in-situ* reduction of Cp_2Co^+ to cobaltocene would enable isolation of pure **2** given the high solubility of cobaltocene in nonpolar solvents. Thus, we treated the as-prepared product mixture with 1 eq. KC_8. While this approach was successful in removing Cp_2Co^+ based on NMR analysis (Figures S16 and S17), this also resulted in greater dissociation of the phosphine oxide ligand. Additional purification steps to remove Cp_2Co and the resulting potassium salts caused further decomposition of **2**. Thus, further analysis of **2** was performed on the co-crystallized mixture of **2** and Cp_2Co^+.

High-resolution mass spectrometry confirms the bulk formulation of complex **2**, which is identified in the full, intact dicationic complex in this spectrum (Figures S18-S20). Notably, the only other significant signal in the mass spectrum is associated with Cp_2Co^+, confirming that the recrystallized product is a mixture of these two complexes with otherwise high purity. Evans NMR method in CD_3CN was performed to estimate the magnetic moment of **2** at 25°C (Figure S12). This analysis is complicated by the fact that the ratio of **2** (paramagnetic) and Cp_2Co^+ (diamagnetic) in the product mixture is difficult to precisely characterize by ^1H NMR. However, based on electrochemical analysis of the recrystallization product (*vide infra*), we estimate a 3:2 ratio of Cp_2Co^+ to **2** in solution (*vide infra*). Using this value to estimate the concentration of **2** in the Evans method samples, the effective magnetic moment is very roughly 6.0 ± 0.4 μB. This estimated range was reproduced over multiple trials. This value is higher than the spin-only value for three unpaired electrons (S = 3/2), which is typical of high-spin Co^{II} centers and may be

ascribed to significant unquenched orbital angular momentum. Thus, despite the large uncertainty associated with the actual concentration of **2** in these samples, this high value for the effective magnetic moment suggests a high-spin Co^{II} description for complex **2**.

Cyclic voltammetry (CV) studies on **2** were performed in acetonitrile to probe its electrochemical properties. As shown in Figure 5, the CV of **2** exhibits vastly different behavior compared to **1**, despite both complexes being formulated as Co^{II} complexes. Complex **2** exhibits an oxidation feature at $E_{p,a}$ = +0.68 V vs $Fc^{+/0}$ (50 mV/s), which is assigned as a metal-centered oxidation to a Co^{III} species. The oxidation wave is chemically irreversible at slower scan rates, but the accompanying reduction wave becomes accessible at faster scan rates. This behavior is consistent with an *EC* mechanism in which a rapid, irreversible chemical step occurs after oxidation at the metal.[44] Scanning the working electrode potential to more negative values, a reversible reduction process is observed at –1.33 V vs $Fc^{0/+}$ (Figure S27).[45] This feature is consistent with the cobaltocenium/cobaltocene redox couple ($Cp_2Co^{+/0}$),[46] which further corroborates our conclusion that cobaltocenium is formed during the aerobic oxidation of **1** (*vide supra*). By comparing the peak heights for the $Cp_2Co^{+/0}$ redox couple to that of the oxidation of **2**, we estimate an approximate 3:2 ratio of these species in this solution.

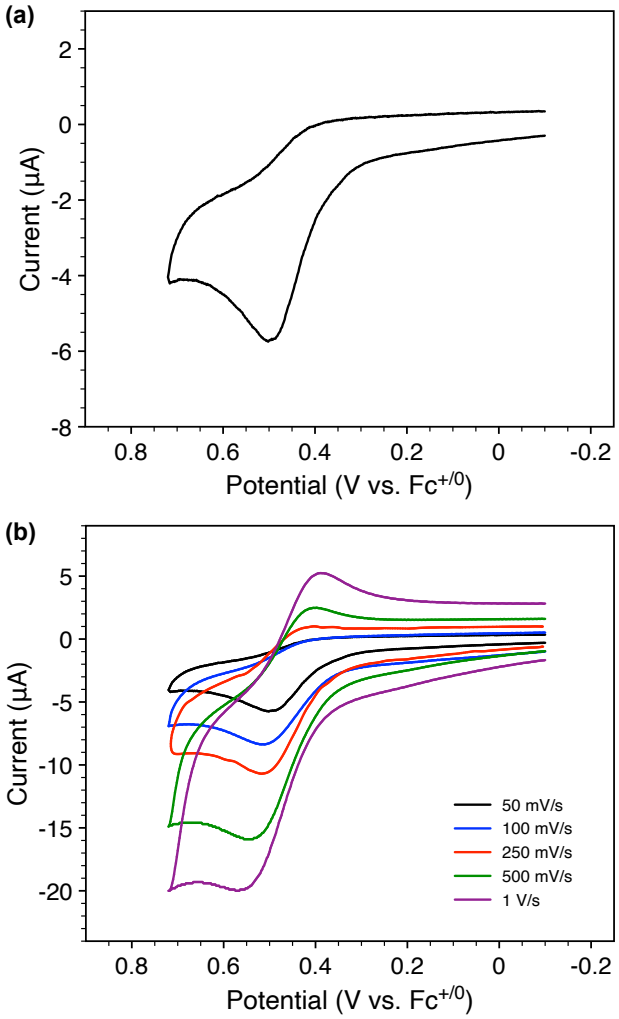

Figure 5. CV of **2** in MeCN (0.1 M [^{n}Bu$_4$N][PF$_6$]) at (a) 50 mV/s, and (b) various scan rates.

The UV-vis absorption behavior of **1** and **2** was also investigated in MeCN solution. The absorption spectrum of **1** shows two main absorbances at 366 and 655 nm (Figure 6a). When this solution in exposed to air, the features associated with **1** disappear and two new absorbance features emerge at 405 nm and 525 nm (Figure 6b). The former is assigned as the main visible transition for the cobaltocenium cation, while the latter is attributed to **2**. For comparison, the UV-vis spectrum of [Cp$_2$Co][PF$_6$] is shown as the red trace in Figure 6b, which corroborates the assignment of the 405 nm absorbance to Cp$_2$Co$^+$. In addition, we further confirm the limited stability of **2** in solution by this method: the absorbances associated with **2** decrease in intensity over several hours and are not replaced by new absorbances in the visible region, consistent with the degradation of the metal complex via loss of the phosphine oxide ligand (Figure S25).

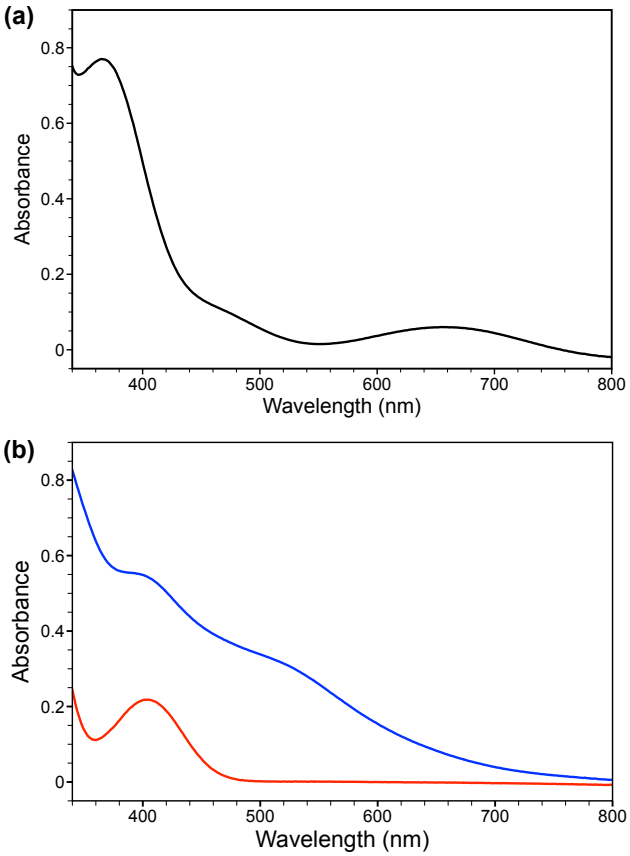

Figure 6. Electronic absorption spectra in MeCN of (a) **1** under N_2, and (b) after air exposure. Initial [**1**] = 0.38 mM. The red trace shows the electronic absorption spectrum of an independently prepared $[Cp_2Co][PF_6]$ solution in MeCN.

Overall, it is evident that the reaction of **1** with oxygen results in oxidation of the phosphine ligand, leading to a dramatic change in the coordination environments at cobalt through ligand exchange. The direct redox reaction between **1** and oxygen via outer-sphere electron transfer is unlikely to initiate this process given the difference in the redox potentials for the oxidation of **1** and the reduction of O_2 in organic solvent.[47] However, the Co^{II} center in **1** may be accessible for O_2 reactivity by an inner-sphere mechanism. Dempsey and co-workers have probed the equilibrium binding of MeCN solvent to related $[CpCo^{II}(P\text{-}P)]^+$ complexes, showing that coordination to Co^{II} is uphill but accessible.[27] Thus, the two-legged piano-stool geometry allows the coordinatively-unsaturated Co^{II} center to interact with solvents, or perhaps substrates. As such, O_2 may interact with the metal in an initial step.[48-50] The analogous behavior with O_2 is not

observed at [Co^{III}], which exists in an air-stable, coordinatively saturated, three-legged piano geometry. The [Co^{I}] complex is air sensitive, although the outcome of this reactivity is unclear: outer-sphere electron transfer with O_2 is feasible based on the relevant redox potentials, which may result in multiple products. As noted above, a related Ni^{II}-P_2N_2 was reported to react with O_2 to generate a similar complex, [Ni^{II}-PO].[24] In this case, the initial reaction of $[Ni(P^{Ph}{}_2N^{Bn}{}_2)_2]^{2+}$ with H_2 is required, which generates Ni^0 species that undergo oxidation to form the phosphine oxide. These results suggest a general reactivity profile for the P_2N_2 ligands in low-valent first-row transition metal complexes in the presence of oxygen, and this deactivation pathway should be considered when evaluating the catalytic activity and lifetimes of such systems.

The reactivity of complex **1** in air is a novel demonstration of facile ligand exchange induced by aerobic oxidation of the original metal complex. The phosphine oxide ligand in **2** does not exhibit strong coordinating ability (the stability of [Ni^{II}-PO] was not reported), and thus dissociation and structural reorganization involving this ligand is reasonable. While the Cp scaffold is often considered to be a strongly coordinating and robust ancillary ligand, its reactivity and lability has been demonstrated in many cases.[51-54] Wiedner and co-workers mention in passing that Cp_2Co^+ is formed as a minor product during the synthesis of their $[^{R}CpCo^{II}(P^{tBu}{}_2N^{Ph}{}_2)]^+$ complexes. In our case, exchange of the $O_2P_2N_2$ and Cp ligands at Co^{II} may initially generate cobaltocene (Cp_2Co^{II}), which would be readily oxidized to the Co^{III} state under aerobic conditions.

CONCLUSION

In summary, we prepared a cyclopentadienyl cobalt(II) complex bearing a P_2N_2 phosphine ligand that reacts with air to generate complex **2** containing two phosphine oxide ligands. Oxidation of the P_2N_2 ligands is accompanied by Cp loss from the cobalt center, which results in the formation of the cobaltocenium cation as the co-product of this oxidation process via ligand exchange. The structure of complex **2** was unambiguously determined by X-ray crystallography and mass spectrometry analysis, confirming its formulation as a dicationic cobalt(II) species with two *fac*-coordinating $O_2P_2N_2$ ligands. This study highlights the ability of the P_2N_2 scaffold to be selectively oxidized to the corresponding phosphine oxide while bound to cobalt(II), which may be a general feature of low-valent metal-P_2N_2 complexes. These results provide useful insights for the design of phosphine ligands for air-tolerant or aerobic catalysis.

EXPERIMENTAL SECTION

Materials and Methods. All work was performed under an inert atmosphere inside a Vacuum Atmospheres glovebox or using standard Schlenk techniques, unless otherwise specified. Acetonitrile and tetrahydrofuran were dried using a Pure Process Technology Solvent Purification System and then dried further over 3 Å molecular sieves. Diethyl ether was dried over 3Å molecular sieves. Acetonitrile-d_3 (99.8% D, Cambridge Isotope Laboratories) was dried over 3Å molecular sieves. All solvents were degassed by three freeze-pump-thaw cycles and stored under an inert atmosphere. Silver hexafluorophosphate ($AgPF_6$) and potassium graphite (KC_8) were purchased from Strem and used as received. Cobaltocenium hexafluorophosphate was purchased from Sigma-Aldrich and used as received. Ferrocene (Fc) was purchased from Sigma-Aldrich and recrystallized from hexanes prior to use. Tetra-*n*-butylammonium hexafluoro-phosphate ($[^nBu_4N][PF_6]$) was purchased from Sigma-Aldrich, recrystallized from ethanol, and dried under vacuum for at least 48 h prior to use. $[CpCo(P^{Ph}_2N^{Bn}_2)(MeCN)][PF_6]_2$ was synthesized according to previously reported procedures.[29]

NMR spectra were collected at 25°C unless otherwise indicated. ^1H and $^{31}P\{^1H\}$ NMR spectra were recorded on a Varian VNMRS 500 MHz spectrometer. The chemical shifts of ^1H and ^{31}P nuclei are reported in parts per million (ppm, δ). The chemical shifts are referenced to the residual solvent peaks (^1H NMR) or phosphoric acid (H_3PO_4). Electronic absorption spectra were recorded on an Agilent Cary 60 UV-vis spectrophotometer with Cary WinUV software using a 1 cm path length quartz cuvette. High resolution mass spectra (HRMS) were collected using an electrospray ionization (ESI) source on positive ion mode with a Xevo™ G2-XS QTof mass spectrometer.

X-ray Crystallography. Single crystal structure determination was performed on a Rigaku XTALab Synergy-S single crystal diffractometer equipped with a HyPix-6000HE area detector (hybrid photo counting) using a Kappa 4-circle goniometer with Cu/Kα radiation (λ = 1.54184 Å). and the CrysAlisPRO software.[55] Single crystals were immersed in oil and mounted on a cryo-loop, and all data were collected at 100(1) K using an Oxford nitrogen gas 800 Series cryostream system. The X-ray data were corrected for Lorentz effects and polarization. Multi-scan or Gaussian absorption corrections were applied in the CrysAlixPRO program. The structures were solved by an intrinsic phasing with SHELXT.[56] Structure refinement program SHELXL was used and supplied all atomic scattering factors.[57] The sp^3 or sp^2 H atoms were placed on calculated (riding

on C atom) positions by use of appropriate SHELXL instructions. Additional crystallographic data and final R indices are given in Table S1. All structures have been deposited into the Cambridge Structural Database (CCDC 2357495 and 2357496).

Cyclic Voltammetry. Cyclic voltammetry (CV) studies were performed using a BASi Epsilon EClipse potentiostat, and the data were processed using BASi Epsilon-EC software (version 2.13.77). All experiments were performed under N_2 in a 20 mL glass vial with a glassy carbon (GC) working electrode (3 mm diameter, BASi), Pt wire counter electrode, and $Ag/AgNO_3$ reference electrode (BASi). The GC electrode was polished with alumina (0.05 µm, BASi) prior to use. CV solutions were typically composed of 1 mM analyte and 0.1 M [^{n}Bu$_4$N][PF_6] in acetonitrile. All potentials are referenced to the $Fc^{+/0}$ couple using ferrocene as an internal standard. Redox couples that exhibited behavior similar to the $Fc^{+/0}$ couple were considered reversible.

Synthesis of [$CpCo^{II}(P^{Ph}_2N^{Bn}_2)$][$PF_6$] (1). [$CpCo^{III}(P^{Ph}_2N^{Bn}_2)(MeCN)$][$PF_6$]$_2$ (133 mg, 0.14 mmol, 1.0 eq) was combined with KC_8 (38 mg, 0.28 mmol, 2.0 eq) in acetonitrile (5 mL). The reaction mixture was stirred for 5 min at 25°C, after which the solution was filtered over celite to remove graphite. The solvent was removed *in vacuo* and a dark red residue was obtained. The [$CpCo^{I}(P^{Ph}_2N^{Bn}_2)$] product was extracted into toluene and the solvent was removed *in vacuo* once again. Characterization of this complex by ^{1}H and ^{31}P NMR is consistent with reported data.[29] This complex can be stored under inert atmosphere or used directly in the next step. A solution of $AgPF_6$ (32 mg, 0.13 mmol, 0.9 eq) in acetonitrile (5 mL) was added to [$CpCo^{I}(P^{Ph}_2N^{Bn}_2)$]. The resulting solution was stirred for 5 min 25°C. The solution was filtered, and the filtrate was evaporated to dryness to obtain **1** as an olive green solid. The crude product was recrystallized from acetonitrile/diethyl ether (1:5) at −35°C. Yield 32.5 mg (42%). ^{1}H NMR (500 MHz, 25ºC, CD_3CN): δ 11.86, 9.56, 8.63, 6.94, 6.38, 0.88. ^{31}P{^{1}H} NMR (202 MHz, 25ºC, CD_3CN): δ -144.71 (sept). HRMS: Calcd for $C_{35}H_{37}ClCoN_2P_2$ ([**1** + Cl]$^+$): *m/z* 641.1453. Found: *m/z* 641.1807. Effective Magnetic Moment: μ_{eff} = 1.84 µB (Evans method).

Preparation of Complex 2. *Representative Procedure.* Complex **1** (150 mg, 0.20 mmol) was dissolved in acetonitrile (5 mL) under inert atmosphere. The solution was exposed to air, resulting in an immediate color change from green to dark orange. The solution was stirred for a further 5 min, after which the solvent was concentrated to ca. 1 mL volume and diethyl ether (20 mL) was added to precipitate the product as a dark yellow solid. The solid was collected by filtration, washed with diethyl ether (3 × 10 mL), and dried under vacuum overnight. ^{1}H NMR

(500 MHz, 25ºC, CD_3CN): δ 60.47, 38.21, 22.59, 19.24, 14.59, 13.07, 11.39, 8.10, 7.38, 6.73, -4.18, -4.78, -25.51, -65.38, -75.94. $^{31}P\{^1H\}$ NMR (202 MHz, 25ºC, CD_3CN): δ -144.61 (sept). HRMS: Calcd for $C_{60}H_{64}CoN_4O_4P_4$ ($[\mathbf{2} - 2PF_6]^{2+}$): *m/z* 543.6600. Found: *m/z* 543.6844. Effective Magnetic Moment: μ_{eff} = ca. 6.0 ± 0.4 μB (Evans method).

ASSOCIATED CONTENT

Supporting Information

The following files are available free of charge.

- Crystallographic details, additional spectroscopic and electrochemical data (PDF)

Accession Codes

CCDC 2357495 and 2357496 contain the supplemental crystallographic data for this paper. These data can be obtained free of charge via www.ccdc.cam.ac.uk/data_request/cif, or by emailing data_request@ccdc.cam.ac.uk, or by contacting The Cambridge Crystallographic Data Centre, 12 Union Road, Cambridge CB2 1EZ, UK; fax: +44 1223 336033.

AUTHOR INFORMATION

Corresponding Author

Kate M. Waldie – Department of Chemistry and Chemical Biology, Rutgers, The State University of New Jersey, New Brunswick, New Jersey 08903, United States; orcid.org/0000-0001-6444-6122; Email: kate.waldie@rutgers.edu

Authors

Sriram Katipamula - Department of Chemistry and Chemical Biology, Rutgers, The State University of New Jersey, New Brunswick, New Jersey 08903, United States; orcid.org/0000-0003-2462-5964

Thomas J. Emge - Department of Chemistry and Chemical Biology, Rutgers, The State University of New Jersey, New Brunswick, New Jersey 08903, United States

Author Contributions

Conceptualization, S.K. and K.M.W.; methodology, S.K. and K.M.W.; investigation, S.K. and T.J.E.; writing – original draft, S.K. and K.M.W.; writing – review and editing; S.K. and K.M.W.; supervision, K.M.W.

Notes

The authors declare no competing financial interests.

ACKNOWLEDGMENTS

This work was supported by Rutgers, The State University of New Jersey. The Rigaku SYNERGY-S X-ray diffractometer was partially funded by an NSF MRI Award (CHE-2117792) to the Rutgers University Department of Chemistry and Chemical Biology.

References

1. Adrio, L. A.; Hii, K. K., Application of phosphine ligands in organic synthesis. *Organomet. Chem* **2009,** *35*, 62-92. DOI: 10.1039/b801380m.
2. Clevenger, A. L.; Stolley, R. M.; Aderibigbe, J.; Louie, J., Trends in the Usage of Bidentate Phosphines as Ligands in Nickel Catalysis. *Chem. Rev.* **2020,** *120* (13), 6124-6196. DOI: 10.1021/acs.chemrev.9b00682.
3. Pignolet, L., *Homogeneous Catalysis with Metal Phosphine Complexes*. Plenum Press: New York, NY, 1983.
4. Phanopoulos, A.; Long, N. J.; Miller, P. W., Triphosphine Ligands: Coordination Chemistry and Recent Catalytic Applications. In *The Chemical Bond III. Structure and Bonding*, Mingos, D., Ed. Springer: 2016; Vol. 171.
5. Spessard, G. O.; Miessler, G. L., *Organometallic Chemistry*. Prentice-Hall: Upper Saddle River, NJ, 1997.

6. Crabtree, R. H., *The Organometallic Chemistry of the Transition Metals*. 5th ed.; John Wiley and Sons: 2009.

7. Fey, N.; Orpen, A. G.; Harvey, J. N., Building ligand knowledge bases for organometallic chemistry: Computational description of phosphorus(III)-donor ligands and the metal–phosphorus bond. *Coord. Chem. Rev.* **2009,** *253* (5-6), 704-722. DOI: 10.1016/j.ccr.2008.04.017.

8. Wiedner, E. S.; Appel, A. M.; Raugei, S.; Shaw, W. J.; Bullock, R. M., Molecular Catalysts with Diphosphine Ligands Containing Pendant Amines. *Chem. Rev.* **2022,** *122* (14), 12427-12474. DOI: 10.1021/acs.chemrev.1c01001.

9. Buckler, S. A., Autoxidation of Trialkylphosphines. *J. Am. Chem. Soc.* **1962,** *84* (16), 3093-3097. DOI: 10.1021/ja00875a011.

10. Barder, T. E.; Buchwald, S. L., Rationale Behind the Resistance of Dialkylbiaryl Phosphines toward Oxidation by Molecular Oxygen. *J. Am. Chem. Soc.* **2007,** *129* (16), 5096-5101. DOI: 10.1021/ja0683180.

11. Cavani, F.; Teles, J. H., Sustainability in Catalytic Oxidation: An Alternative Approach or a Structural Evolution? *ChemSusChem* **2009,** *2* (6), 508-534. DOI: 10.1002/cssc.200900020.

12. Tereniak, S. J.; Landis, C. R.; Stahl, S. S., Are Phosphines Viable Ligands for Pd-Catalyzed Aerobic Oxidation Reactions? Contrasting Insights from a Survey of Six Reactions. *ACS Catal.* **2018,** *8* (4), 3708-3714. DOI: 10.1021/acscatal.8b01009.

13. Wright, A. M.; Pahls, D. R.; Gary, J. B.; Warner, T.; Williams, J. Z.; Knapp, S. M. M.; Allen, K. E.; Landis, C. R.; Cundari, T. R.; Goldberg, K. I., Experimental and

Computational Investigation of the Aerobic Oxidation of a Late Transition Metal-Hydride. *J. Am. Chem. Soc.* **2019,** *141* (27), 10830-10843. DOI: 10.1021/jacs.9b04706.

14. Phearman, A. S.; Ardon, Y.; Goldberg, K. I., Insertion of Molecular Oxygen into a Gold(III)–Hydride Bond. *J. Am. Chem. Soc.* **2024,** *146* (6), 4045-4059. DOI: 10.1021/jacs.3c12285.

15. Klotz, I. M.; Kurtz Jr, D. M., Metal-dioxygen complexes: A perspective. *Chem. Rev.* **1994,** *94* (3), 567-568. DOI: 10.1021/cr00027a001.

16. Ortiz de Montellano, P. R., Hydrocarbon Hydroxylation by Cytochrome P450 Enzymes. *Chem. Rev.* **2010,** *110* (2), 932-948. DOI: 10.1021/cr9002193.

17. Krebs, C.; Galonić Fujimori, D.; Walsh, C. T.; Bollinger, J. M., Jr., Non-Heme Fe(IV)–Oxo Intermediates. *Acc. Chem. Res.* **2007,** *40* (7), 484-492. DOI: 10.1021/ar700066p.

18. Scheuermann, M. L.; Goldberg, K. I., Reactions of Pd and Pt Complexes with Molecular Oxygen. *Chem. Eur. J.* **2014,** *20* (45), 14556-14568. DOI: 10.1002/chem.201402599.

19. Wakerley, D. W.; Reisner, E., Oxygen-tolerant proton reduction catalysis: much O2 about nothing? *Energy Environ. Sci.* **2015,** *8* (8), 2283-2295. DOI: 10.1039/C5EE01167A.

20. Mondal, B.; Dey, A., Development of air-stable hydrogen evolution catalysts. *Chem. Commun.* **2017,** *53* (55), 7707-7715. DOI: 10.1039/C7CC02941A.

21. Loginov, D. A.; Shul'pina, L. S.; Muratov, D. V.; Shul'pin, G. B., Cyclopentadienyl cobalt(III) complexes: Synthetic and catalytic chemistry. *Coord. Chem. Rev.* **2019,** *387*, 1-31. DOI: 10.1016/j.ccr.2019.01.022.

22. Koelle, U.; Paul, S., Electrochemical reduction of protonated cyclopentadienylcobalt phosphine complexes. *Inorg. Chem.* **1986,** *25* (16), 2689-2694. DOI: 10.1021/ic00236a007.

23. Nagasawa, T.; Nagata, T., Synthesis and electrochemistry of Co (III) and Co (I) complexes having C5Me5 auxiliary. *Biochim. Biophys. Acta, Bioenerg.* **2007,** *1767* (6), 666-670. DOI.

24. Fang, M.; Wiedner, E. S.; Dougherty, W. G.; Kassel, W. S.; Liu, T.; DuBois, D. L.; Bullock, R. M., Cobalt Complexes Containing Pendant Amines in the Second Coordination Sphere as Electrocatalysts for H2 Production. *Organometallics* **2014,** *33* (20), 5820-5833. DOI: 10.1021/om5004607.

25. Roy, S.; Sharma, B.; Pécaut, J.; Simon, P.; Fontcave, M.; Tran, P. D.; Derat, E.; Artero, V., Molecular Cobalt Complexes with Pendant Amines for Selective Electrocatalytic Reduction of Carbon Dioxide to Formic Acid. *J. Am. Chem. Soc.* **2017,** *139* (10), 3685-3696. DOI: 10.1021/jacs.6b11474.

26. Elgrishi, N.; Kurtz, D. A.; Dempsey, J. L., Reaction Parameters Influencing Cobalt Hydride Formation Kinetics: Implications for Benchmarking H2-Evolution Catalysts. *J. Am. Chem. Soc.* **2017,** *139* (1), 239-244. DOI: 10.1021/jacs.6b10148.

27. Kurtz, D. A.; Dhar, D.; Elgrishi, N.; Kandemir, B.; McWilliams, S. F.; Howland, W. C.; Chen, C.-H.; Dempsey, J. L., Redox-Induced Structural Reorganization Dictates Kinetics of Cobalt(III) Hydride Formation via Proton-Coupled Electron Transfer. *J. Am. Chem. Soc.* **2021,** *143* (9), 3393-3406. DOI: 10.1021/jacs.0c11992.

28. Cook, A. W.; Emge, T. J.; Waldie, K. M., Insights into Formate Oxidation by a Series of Cobalt Piano-Stool Complexes Supported by Bis(phosphino)amine Ligands. *Inorg. Chem.* **2021,** *60* (10), 7372-7380. DOI: 10.1021/acs.inorgchem.1c00563.

29. Katipamula, S.; Cook, A. W.; Niedzwiecki, I.; Emge, T. J.; Waldie, K. M., Electrocatalytic Formate Oxidation by Cobalt-Phosphine Complexes. *ChemRxiv* **2023**. DOI: 10.26434/chemrvix-2023-tfn6t.

30. Harlow, R. L.; McKinney, R. J.; Whitney, J. F., Paramagnetic Organometallic Complexes. Comparison of Geometric and Electronic Structures of Paramagnetic Bis(triethylphosphine)cyclopentadienylcobalt(11) Tetrafluoroborate and Diamagnetic Bis(triethylphosphine)cyclopentadienylcobalt(I). *Organometallics* **1983,** *2* (12), 1839-1842. DOI: 10.1021/om50006a023.

31. Kurtz, D. A.; Dempsey, J. L., Proton-Coupled Electron Transfer Kinetics for the Photoinduced Generation of a Cobalt(III)-Hydride Complex. *Inorg. Chem.* **2019,** *58* (24), 16510-16517. DOI: 10.1021/acs.inorgchem.9b02445.

32. Rheingold, A. L.; Liable-Sands, L. M.; Trofimenko, S., 4,5-Bis(diphenylphosphinoyl)-1,2,3-triazole: A Powerful New Ligand That Uses Two Different Modes of Chelation. *Angew. Chem. Int. Ed.* **2000,** *39* (18), 3321-3324. DOI: 10.1002/1521-3773(20000915)39:18<3321::AID-ANIE3321>3.0.CO;2-V.

33. Siefert, R.; Weyhermüller, T.; Chaudhuri, P., Isolation, structural and spectroscopic investigations of complexes with tridentate [O,P,O] and [O,O,O] donor ligands. *J. Chem. Soc., Dalton Trans.* **2000,** *2000* (24), 4656-4663. DOI: 10.1039/B005693F.

34. Courtney, D.; Müller-Bunz, H.; Manning, A. R., [Co{Ph2P(O)CH2P(O)Ph2}3][CoCl4] · 8CHCl3: Crystal structure and formation from [Co2(Ph2PCH2PPh2)(CO)6] in chloroform. *Inorg. Chim. Acta* **2006,** *359* (10), 3367-3370. DOI: 10.1016/j.ica.2006.04.001.

35. Kostin, G.; Borodin, A.; Emely'anov, V.; Naumov, D.; Virovets, A.; Rohmer, M.-M.; Varnek, A., Synthesis and structure of heterometallic compounds of [RuNO(NO2)4OH]2− with triphenyl phosphine oxide complexes of Co(II), Ni (II), and Zn(II). *J. Mol. Struct.* **2007,** *837* (1-3), 63-71. DOI: 10.106/j.molstruc.2006.10.004.

36. Dartiguenave, M.; Dartiguenave, Y.; Oliver, M. J.; Beauchamp, A. L., Reaction of [Co(PMe3)4]BPh4 with Oxygen: Crystal and Molecular Structure of [Co(MeCN)2(OPMe3)4](BPh4)2. *J. Coord. Chem.* **2009,** *21* (3), 275-281. DOI: 10.1080/00958979009409726.

37. Lv, Q.-Y.; Lei, W.-J.; Liu, Y.-L.; Zhan, S.-Z.; Ye, J.-S., Reactivity of tetracyanoquinodimethane with cobalt(II) chloride and bis(diphylphospino)methane in air. *Polyhedron* **2010,** *29* (14), 2780-2786. DOI: 10.1016/j.poly.2010.06.031.

38. Stieler, R.; Bublitz, F.; Lang, E. S.; de Oliveira, G. M., Synthesis, structure and optical features of single adamantanoid Hg–SePh–X anionic clusters stabilized by octahedral complexes (Ph = phenyl; X = Cl, Br, I). *Polyhedron* **2012,** *31* (1), 596-600. DOI: 10.1016/j.poly.2011.10.012.

39. Varga, F.; Rajnák, C.; Titiš, J.; Moncol, J.; Boča, R., Slow magnetic relaxation in a Co(ii) octahedral–tetrahedral system formed of a [CoL3]2+ core with L = bis(diphenylphosphanoxido) methane and tetrahedral [CoBr4]2− counter anions. *Dalton Trans.* **2017,** *46* (13), 4148-4151. DOI: 10.1039/C7DT00376E.

40. Luck, R. L.; Maass, J. S.; Newberry, N. K.; Zeller, M., Syntheses, X-ray structure, emission and vibrational spectroscopies, DFT and thermogravimetric studies of two complexes containing the bidentate ligand 5-phenyl-1H-pyrazol-3-yl)methyl) phosphine oxide. *J. Coord. Chem.* **2019,** *72* (15), 2574-2585. DOI: 10.1080/00958972.2019.1674291.

41. Page, S. J.; Rogers-Simmonds, D.; White, A. J. P.; Miller, P. W., Synthesis and crystallographic characterisation of a homologous series of bis-tridentate phosphine oxide NP3O3 Fe(II), Co(II), Ni(II) and Cu(II) complexes. *Inorg. Chim. Acta* **2020,** *512* (2020), 119870. DOI: 10.1016/j.ica.2020.119870.

42. Yang, J. Y.; Bullock, R. M.; Dougherty, W. G.; Kassel, W. S.; Twamley, B.; DuBois, D. L.; Rakowski DuBois, M., Reduction of oxygen catalyzed by nickel diphosphine complexes with positioned pendant amines. *Dalton Trans.* **2010,** *39* (12), 3001-3010. DOI: 10.1039/B921245K.

43. Hilliard, C. R.; Bhuvanesh, N.; Gladysz, J. A.; Blümel, J., Synthesis, purification, and characterization of phosphine oxides and their hydrogen peroxide adducts. *Dalton Trans.* **2012,** *41* (6), 1742-1754. DOI: 10.1039/C1DT11863C.

44. Bard, A. J.; Faulkner, L. R., *Electrochemical Methods: Fundamentals and Applications*. 2nd ed.; John Wiley & Sons: 2001.

45. Bard, A. J.; Garcia, E.; Kukharenko, S.; Strelets, V. V., Electrochemistry of Metallocenes at Very Negative and Very Positive Potentials. Electrogeneration of 17-Electron Cp2Co2+, Cp2Co2-, and Cp2Ni1 2~ Species. *Inorg. Chem.* **1993,** *32* (16), 3528-3531. DOI: 10.1021/ic00068a024.

46. Connelly, N. G.; Geiger, W. E., Chemical Redox Agents for Organometallic Chemistry. *Chem. Rev.* **1996,** *96* (2), 877-910. DOI: 10.1021/cr940053x.

47. Vasudevan, D.; Wendt, H., Electroreduction of oxygen in aprotic media. *J. Electroanal. Chem.* **1995,** *392* (1-2), 69-74. DOI: 10.1016/0022-0728(95)04044-O.

48. Sen, A.; Halpern, J., Role of transition metal-dioxygen complexes in catalytic oxidation. Catalysis of the oxidation of phosphines by dioxygen adducts of platinum. *J. Am. Chem. Soc.* **1977,** *99* (25), 8337-8339. DOI: 10.1021/ja00467a046.

49. Tovrog, B. S.; Kitko, D. J.; Drago, R. S., Nature of the bound oxygen in a series of cobalt dioxygen adducts. *J. Am. Chem. Soc.* **1976,** *98* (17), 5144-5153. DOI: 10.1021/ja00433a016.

50. Tiné, M. R., Cobalt complexes in aqueous solutions as dioxygen carriers. *Coord. Chem. Rev.* **2012,** *256* (1-2), 316-327. DOI: 10.1016/j.ccr.2011.10.009.

51. Crabtree, R. H., The stability of organometallic ligands in oxidation catalysis. *J. Organomet. Chem.* **2014,** *751*, 174-180. DOI: 10.1016/j.jorganchem.2013.07.061.

52. Campos, J.; Hintermair, U.; Brewster, T. P.; Takase, M. K.; Crabtree, R. H., Catalyst Activation by Loss of Cyclopentadienyl Ligands in Hydrogen Transfer Catalysis with Cp*IrIII Complexes. *ACS Catal.* **2014,** *4* (3), 973-985. DOI: 10.1021/cs401138f.

53. Parche, J.; Rupf, S. M.; Sievers, R.; Malischewski, M., Substitution lability of the perfluorinated Cp* ligand in Rh(I) complexes. *Dalton Trans.* **2023,** *52* (17), 5496-5502. DOI: 10.1039/D3DT00425B.

54. VanderWiede, A.; Prokopchuk, D. E., Cyclopentadienyl ring activation in organometallic chemistry and catalysis. *Nat. Rev. Chem.* **2023,** *7*, 561-572. DOI: 10.1038/s41570-023-00501-1.

55. OD, R. *CrysAlis PRO, including ABSPACK.*, Yarnton, England., 2018.

56. Sheldrick, G. M. *ActaCryst.A71,3–8.*, 2015a.

57. Sheldrick, G. M. *ActaCryst.C71,3–8.*, 2015b.